doi:10.1038/nature09446

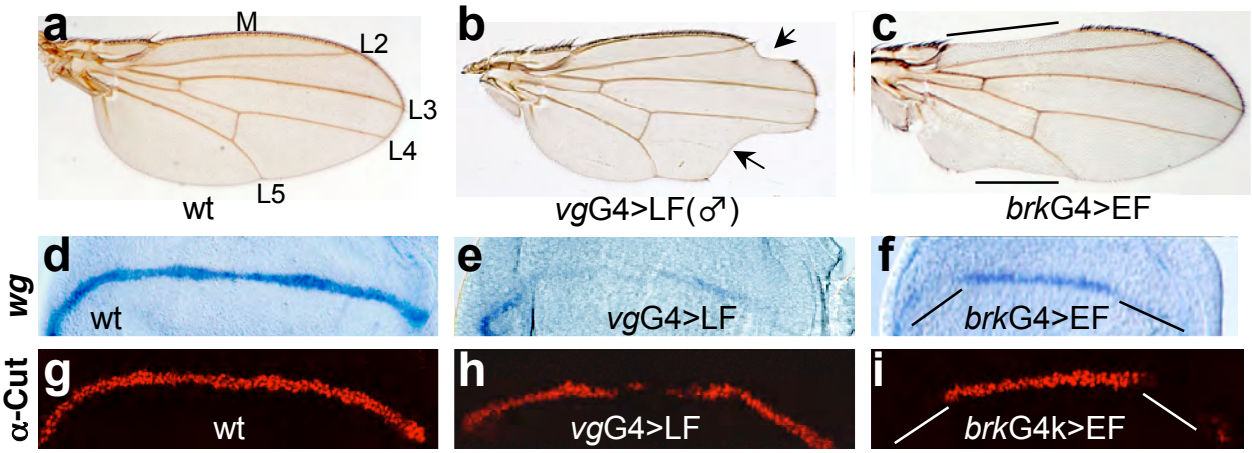

S1: LF and EF inhibit Notch signaling in *Drosophila*

a) A wild-type (wt) adult wing. The margin (M) and longitudinal veins (L2-L5) are indicated.

b) A wing from a *vg*G4>LF male with moderate notching along the wing margin (arrows).

c) A *brk*G4>EF wing exhibiting large notches in extreme anterior and posterior regions (bars) corresponding to where the toxin was expressed during larval stages.

d-f) *wingless* (*wg*) expression along the wing margin in larval imaginal discs: **d)** wild-type, **e**), *vg*G4>LF, **f)** *brk*G4>EF. **g-i**) Cut expression in wing discs: **g)** wild-type, **h)** *vg*G4>LF, **i)** *brk*G4>EF. Bars indicate the domain of GAL4 expression.

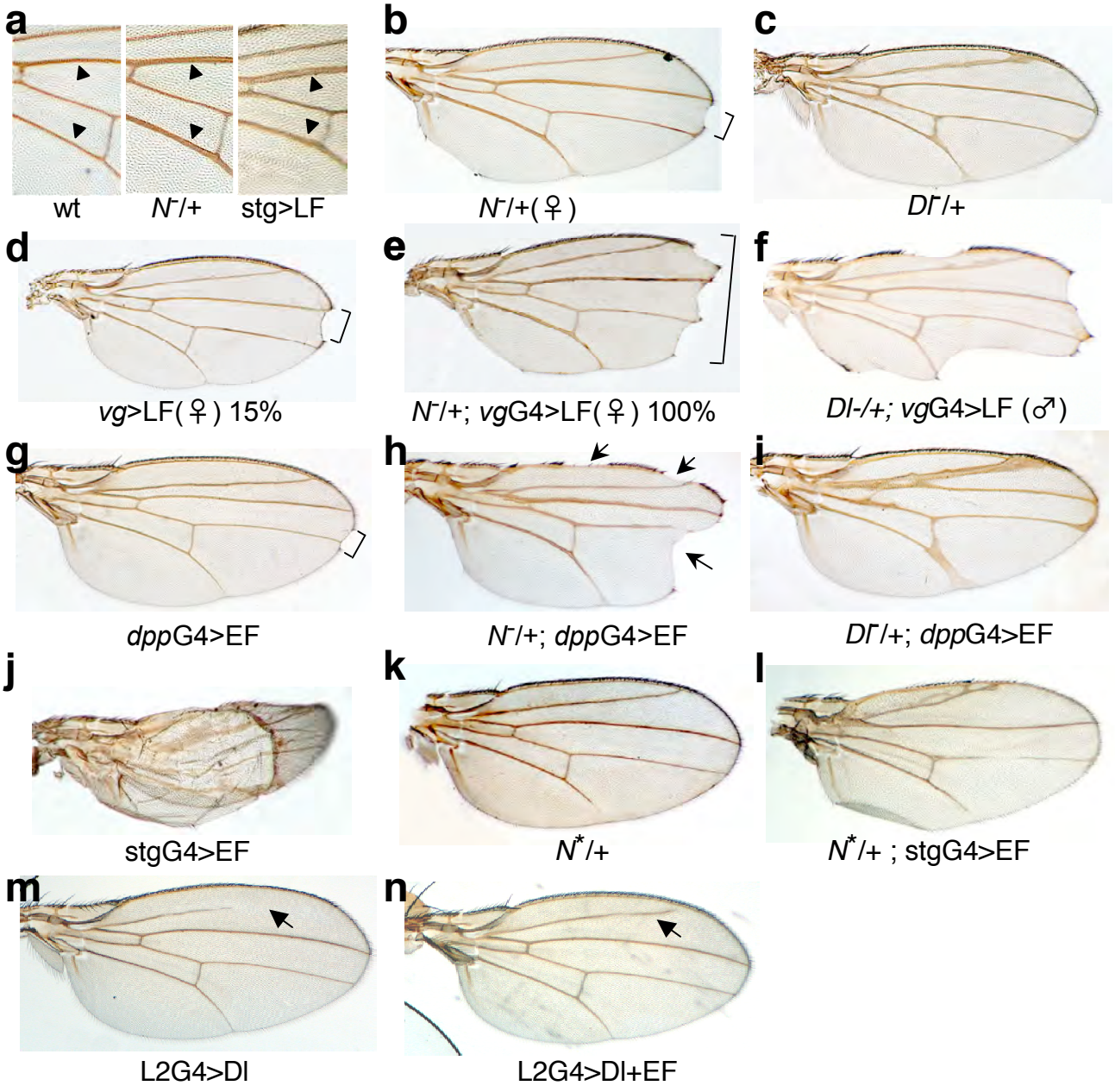

S2: LF and EF interact genetically with Notch pathway components

a) High magnification views of longitudinal veins L2-L5 (arrowheads point at veins L3 and L5) in a wild-type wing (left panel), a N^{-}/+ wing which has thickened veins L3 and L5 (middle panel, arrowheads), and a stgG4>LF3X wing, which also has thickened L3 and L5 veins (right panel, arrowheads: stgG4 = strong ubiquitous expression driven by the MS1096-GAL4 line).

b) A N^{-}/+ wing (bracket shows small notch in margin (N^{-} refers to N^{55e11} in this and subsequent panels). **c**) A heterozygous Dl^{-}/+ wing with moderately thickened L2 and L5 veins (note that there

is no notching of the margin). *Dl*$^{-}$ refers to the *Dl*^{3} allele in experiments shown throughout this figure. **d**) A wing from a *vg*G4>LF female with a small wing notch. Notches are only observed in 15% of females. **e)** A *vg*G4>LF; *N*$^{-}$/+ female wing displaying strong enhancement of the notching phenotype caused by *vg*G4>LF (panel **d**) or by the *N*$^{-}$/+ mutation (panel **b**) alone.

f) A *vg*G4>LF; *Dl*$^{-}$/+ male wing with strong notching. This represents a synergistic interaction as expression of LF in a wild-type disc (Fig. **1b**) has only a moderate phenotype and Dl-/+ individuals (panel **c**) exhibit no notching at all. **g**) A *dpp*G4>EF wing with a small distal wing notch (bracket). **h**) A *N*$^{-}$/+; dppG4>EF wing with greatly enhanced wing notching (arrows) relative to either *dpp*G4>EF or N^{-}/+ individuals. **i**) A *Dl*$^{-}$/+; dppG4>EF wing: EF strongly enhances the *Dl*$^{-}$ thickened vein phenotype. **j**) High level expression of EF in a stgG4>EF wing results in a strong phenotype including thickened veins (arrowhead). **k**) A *N**/+ wing (*N** refers to *N*^{Abx1}, an activated allele of Notch). **l**) A *N**/+; stgG4>EF wing in which activated Notch strongly suppresses the EF phenotype. **m**) An L2G4>Dl wing in which Dl is expressed in the L2 vein primordium (arrow points at a truncation of vein 2 caused by Dl, L2G4 refers to an L2 vein-specific GAL4 driver). **n**) An L2G4>Dl+EF wing (arrow shows that the L2 vein is partially restored, indicating that EF inhibits the effect of mis-expressed Dl).

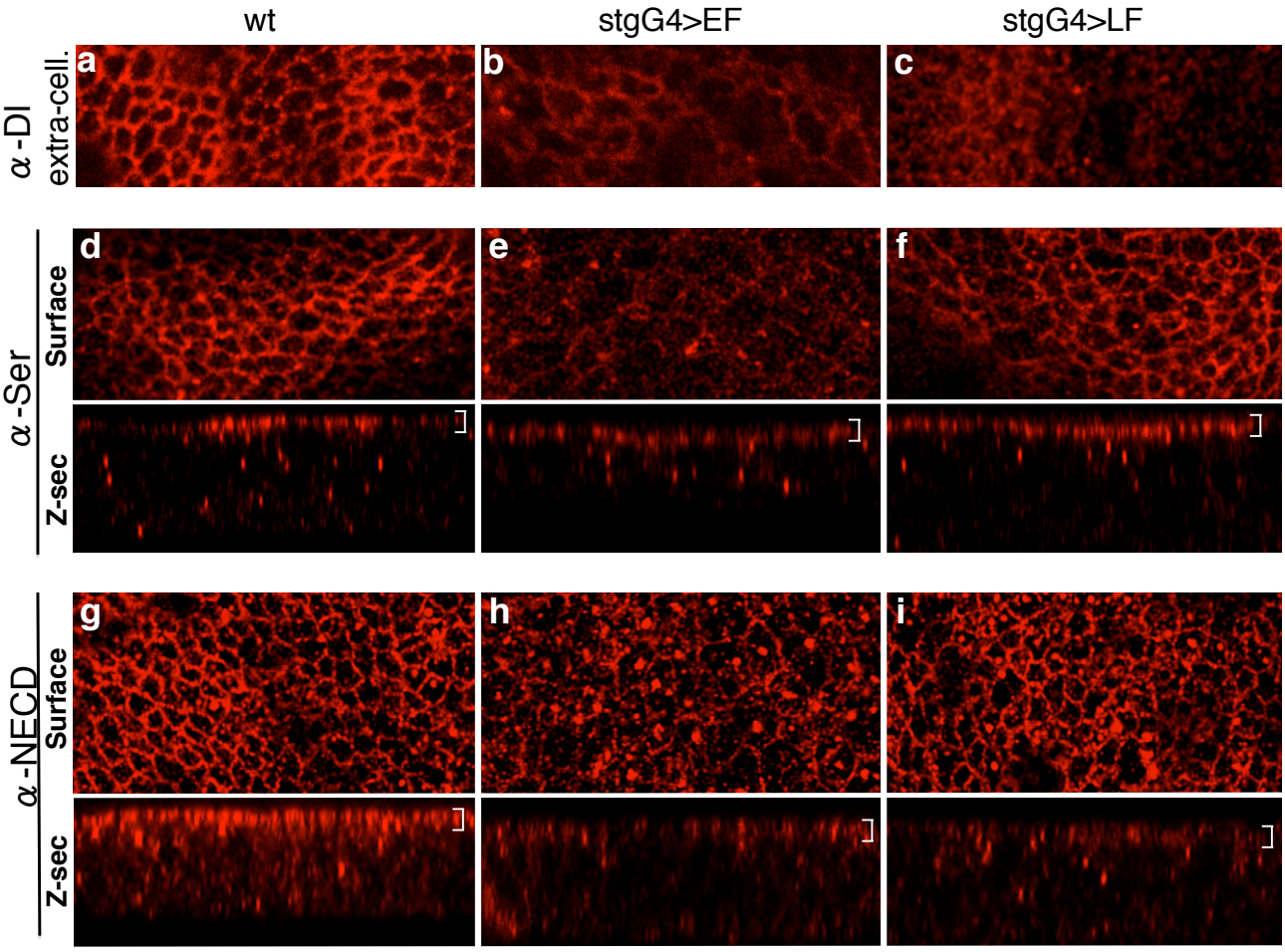

S3: Effects of EF and LF Notch pathway trafficking

a-c) Extracellular staining for Dl in wt (**a**), stgG4>EF (**b**), and stgG4>LF (**c**) wing imaginal discs. The focal plane is at the apical cell surface. **d-f)** Anti-Serrate stains of wt (**d**), stgG4>EF (**e**), and stgG4>LF (**f**) wing discs viewed from a surface perspective (top panels) and as Z-sections (lower panels, brackets indicate apical cell surface). EF expression reduced cell surface levels of Ser (**e**), similar to its effect on Dl (Fig. **1e,g**). In contrast to EF, LF has little if any effect on Ser expression (**f**). **g-i)** Anti-Notch (extracellular domain - ECD) stains of wt (**g**), stgG4>EF (**h**), and stgG4>LF (**i**) wing discs viewed from a surface perspective (top panels) and as Z-sections (lower panels, brackets indicate apical cell surface). Both EF (**h**) and LF (**i**) result in reduced apical levels of Notch.

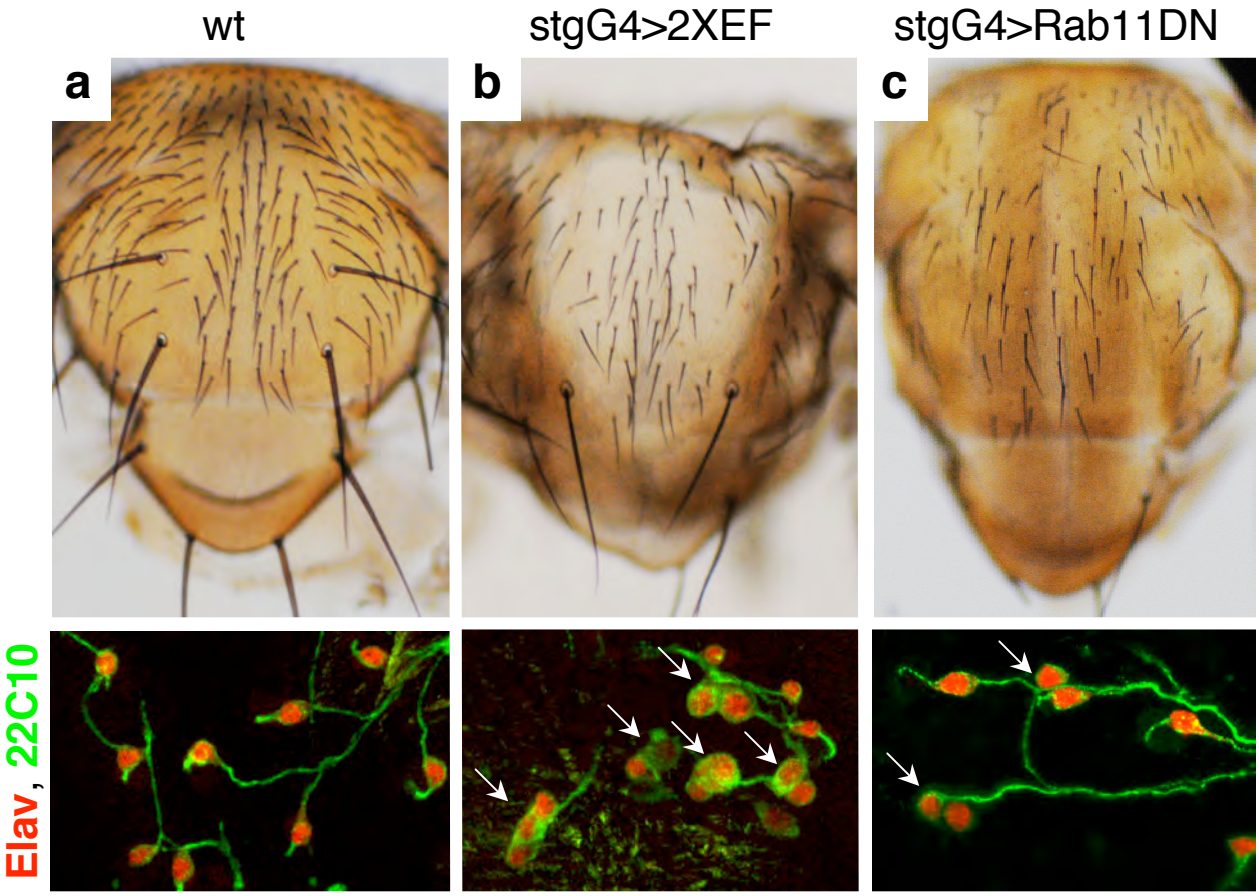

S4: EF and Rab11DN induce Notch-like bristle phenotypes

a-c) Adult thoraxes from wt (**a**), stgG4>2XEF (i.e., two copies of the UAS-EF transgene) (**b**), and stgG4>Rab11DN (**c**) flies (upper panels) and accompanying stains of underlying neurons (lower panels). Both EF (**b**) and Rab11DN (**c**) cause similar reduction in microchaete (small) and macrochaete (large) bristles. This phenotype typically results from inhibiting Notch signaling between secondary sensory organ precursor cells causing the outer precursor cell, which would give rise to the socket and hair, to be transformed into an inner precursor cell, giving rise to neurons and glial cells. This transformation of outer-to-inner precursor cells can be visualized in the lower panels by double staining for 22C10 (green label for neuronal axons) and Elav (red label for neuronal nuclei), which shows a duplication of neurons in thoraxes of stgG4>2XEF (**b**), and stgG4>Rab11DN (**c**) flies instead of single neurons as in wild-type (**a**). Arrows indicate supernumerary neurons.

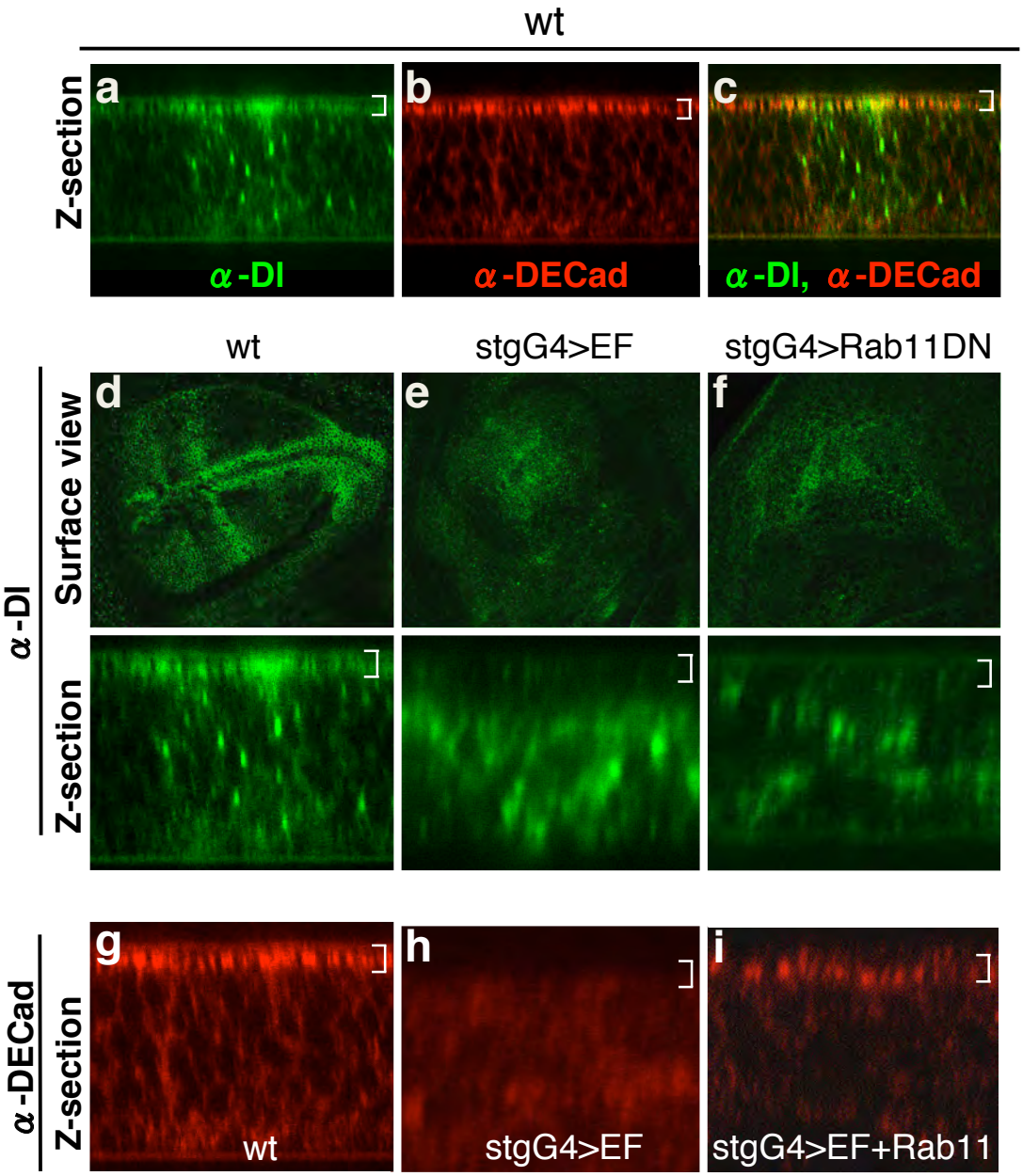

S5: Additional evidence that Rab11 mediates the effect of EF on Dl and DECad

a-c) Co-localization of Dl and DECad at the apical cell surface in a wild-type wing imaginal disc. Z-section of Dl (**a**) and DECad staining (**b**) reveal that these two proteins co-localize (**c**) at the adherens junction (indicated by brackets in all Z-sections). (**d-e**) Expression of EF (**e**) and Rab11DN (**f**) with the stgG4 driver reduce Dl expression at the apical cell surface in a similar fashion (compare with wt in **d**). Upper panels show surface views and lower panels show Z-sections (Note: Z-section in **d** is a higher magnification view of the same disc shown in **a** and Fig. **1p**). Brackets in Z-sections indicate the apical cell surface. **g-i**) DECad expression at the apical cell surface (**g**) is greatly reduced by expression of EF using the stgG4 driver (**h**) and this effect of EF is partially rescued by co-expression of wt Rab11 (**i**). Z-sections are shown. Brackets indicate the apical cell surface.

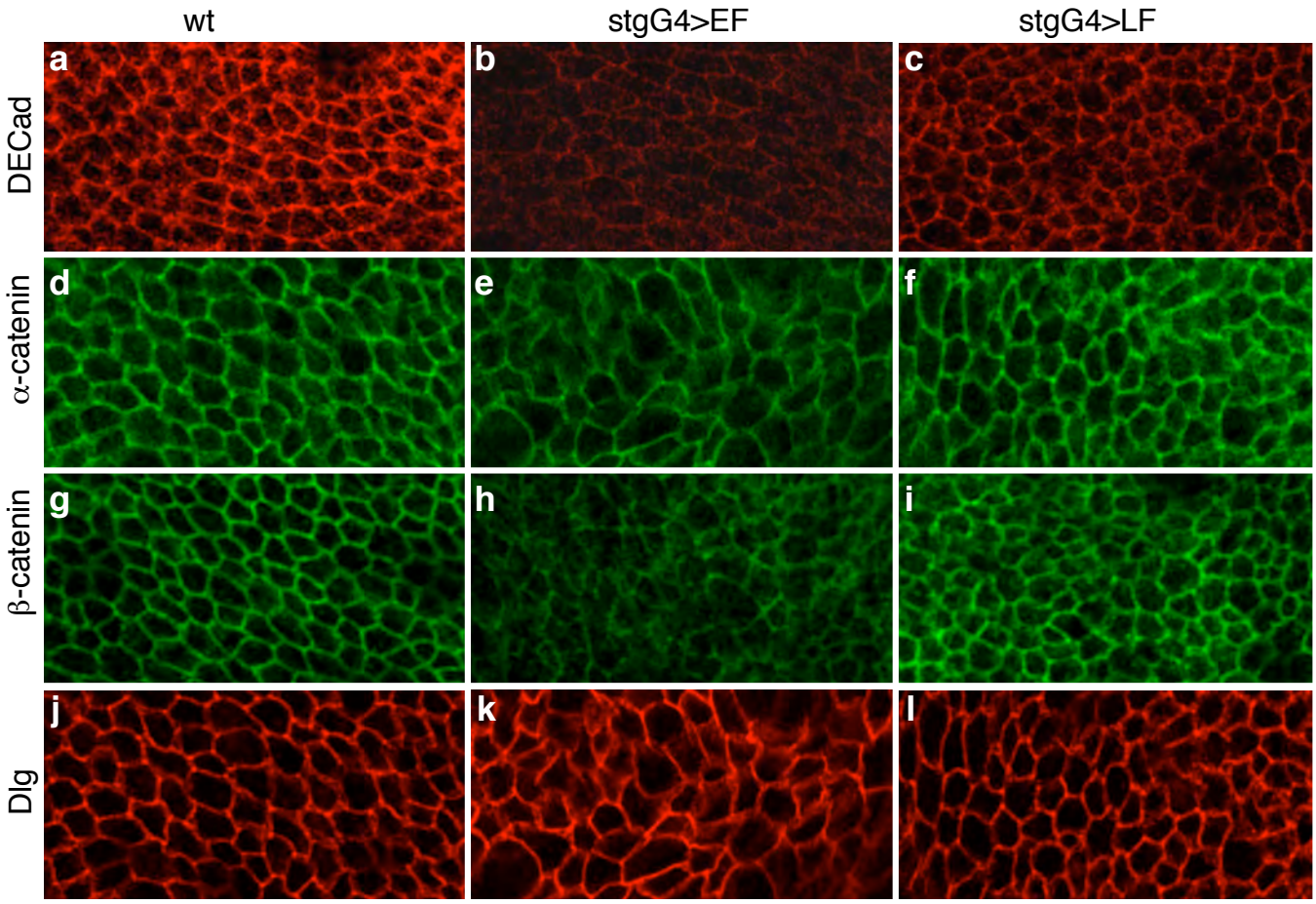

S6: Further analysis of the effects of EF and LF on components of the adherens junction

Expression of various adherens junction (AJ) proteins DECad (**a-c**: **a,b** also shown in Fig. **3d,e**) α-catenin (**d-f**), β-catenin (**g-i**), and Discs-large - Dlg (**j-l**) in wt (**a,d,g,j**), stgG4>EF (**b,e,h,k**), or stgG4>LF (**c,f,i,l**) wing discs. EF reduces expression of both catenins but not Dlg, indicating that the adherens junctions are not simply eliminated by the action of this toxin. LF has a weaker effect on DECad (**c**), and little, if any, effect on the expression of other AJ proteins (**f,i,l**).

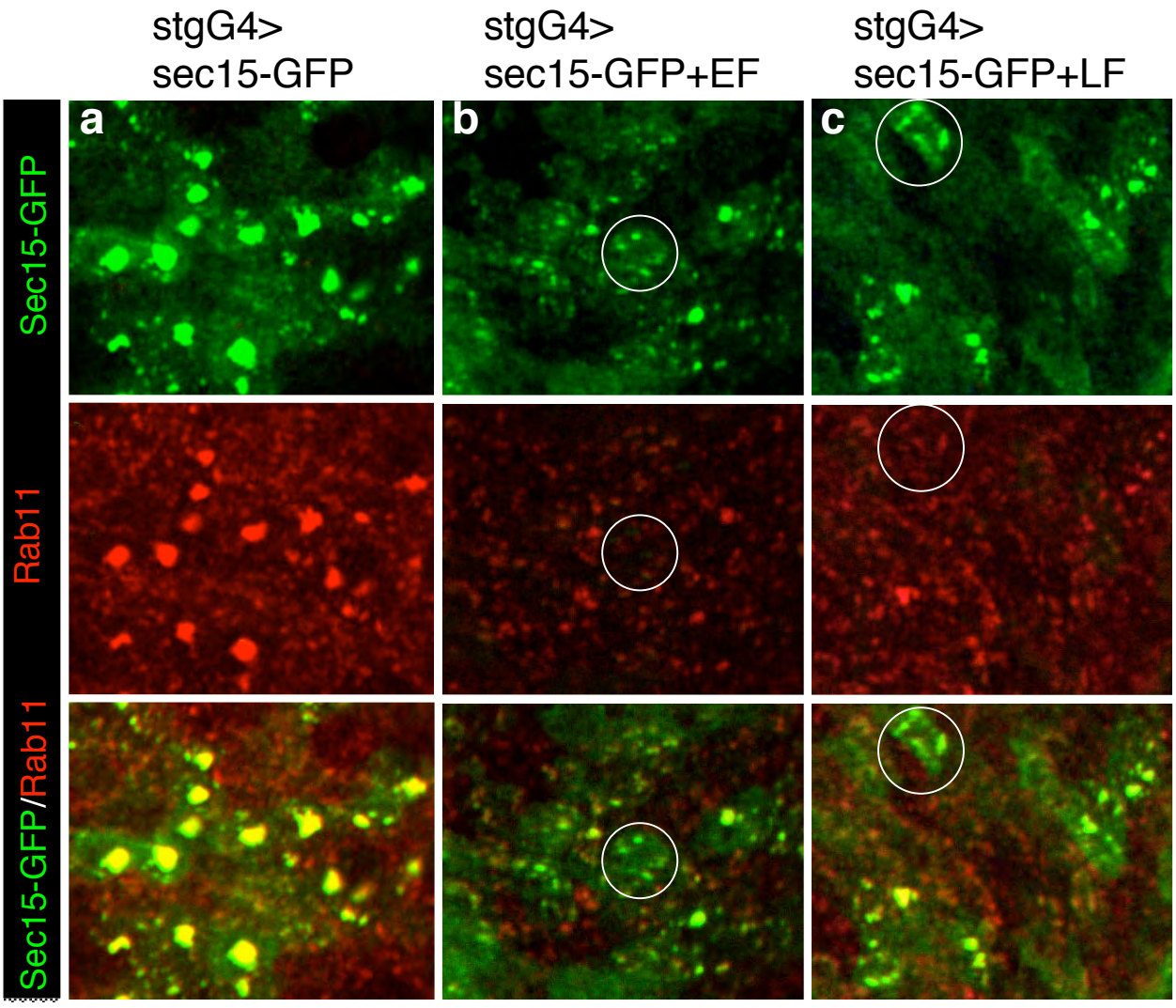

S7: Rab11 levels are reduced in remaining Sec15-GFP vesicles in EF- or LF-expressing discs

Both EF and LF greatly reduce expression of punctate Sec15-GFP staining in wing discs (**b,c**), which in wild-type discs co-localize faithfully with Rab11 (**a**). In addition, the few typically smaller remaining punctae of Sec15-GFP in EF (**b**) or LF (**c**) expressing discs are associated with greatly reduced relative levels of Rab11 (e.g., punctae indicated within circles), suggesting that these two components are no longer linked in proper stoichiometric ratios. Sec15-GFP is shown in green and endogenous Rab11, visualized with an antibody, is shown in red.

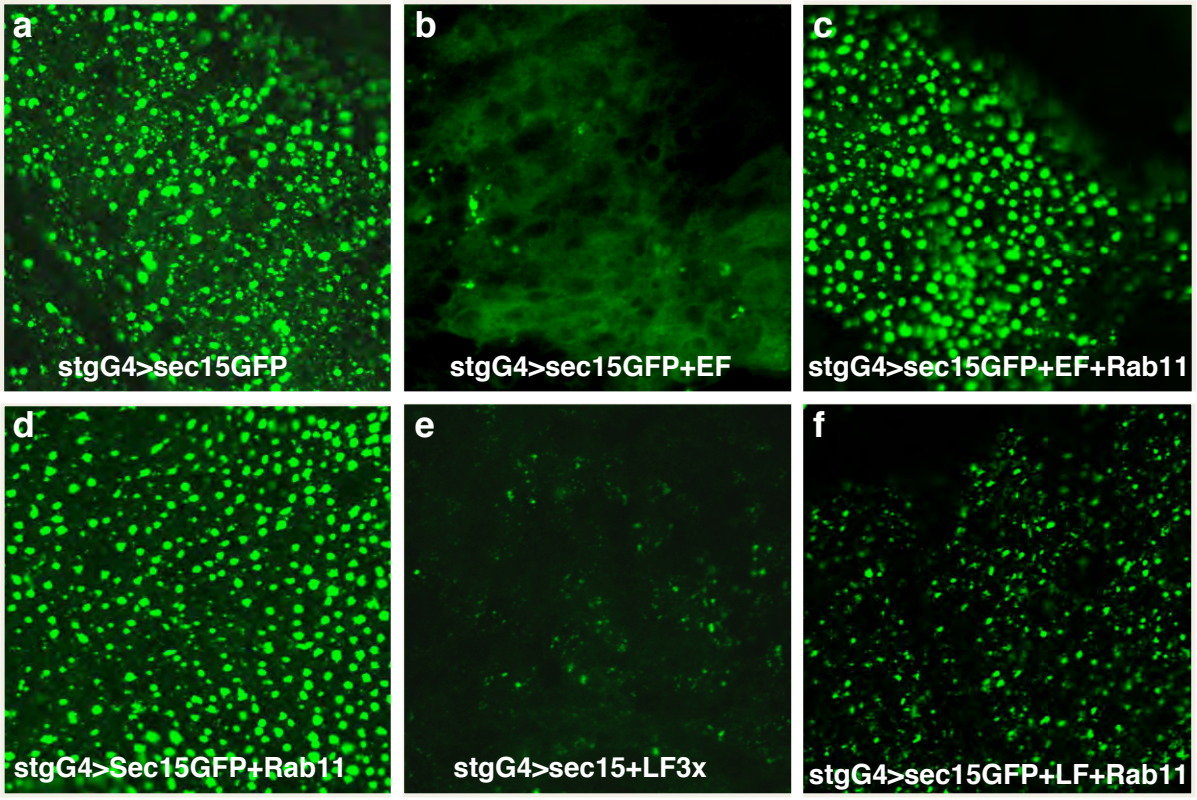

S8: Rab11 rescue of punctate Sec15-GFP expression is much greater for EF than LF

Punctate Sec15-GFP expression in wing discs (**a**), which is greatly reduced by expression of EF (**b**), or LF (**e**), can be fully rescued by co-expression with Rab11wt in the case of EF (**c**), but not LF (**f**). The weak rescue observed in the case of LF (**f**) may be due to endogenous Rab11 levels normally being limiting since the size of Sec15-GFP vesicles also increases in wild-type discs over-expressing Rab11 (**d**). This modest effect does not result in any obvious adult phenotype, however (**Fig. 2m**). All constructs were expressed with the stgG4 driver.

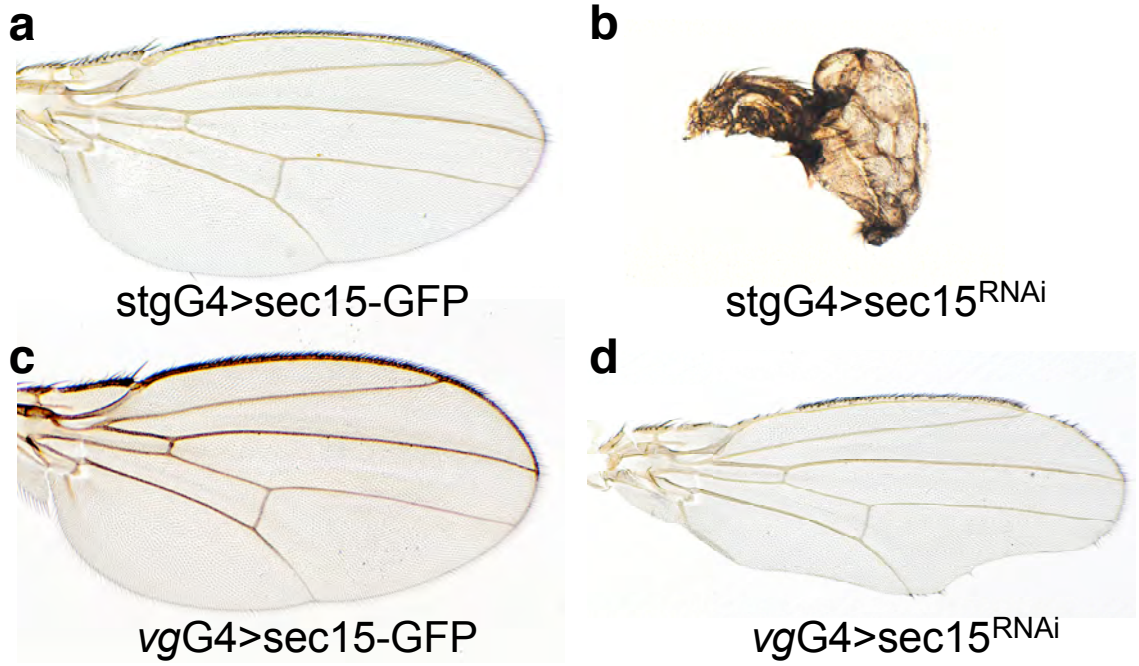

S9: Knock-down of *sec15* causes Notch-like phenotypes

Expression of wild-type (wt) *sec15* results in no obvious wing phenotype with either the strong ubiquitous stgG4 (**a**) or wing margin *vg*G4 (**c**) drivers. Expression of the a *sec15*-RNAi construct with the stgG4 driver, however, results in very small wings with extra veins (**b**), resembling the synergistic effect caused by expressing EF+LF with that same driver (**Fig. 2k**), or a notched wing margin using *vg*G4 (**d**), which also is similar to the phenotype caused by expression of LF with the same driver (**Fig. 1b**). EF also produces similar notching with the *vg*G4 driver (data not shown).

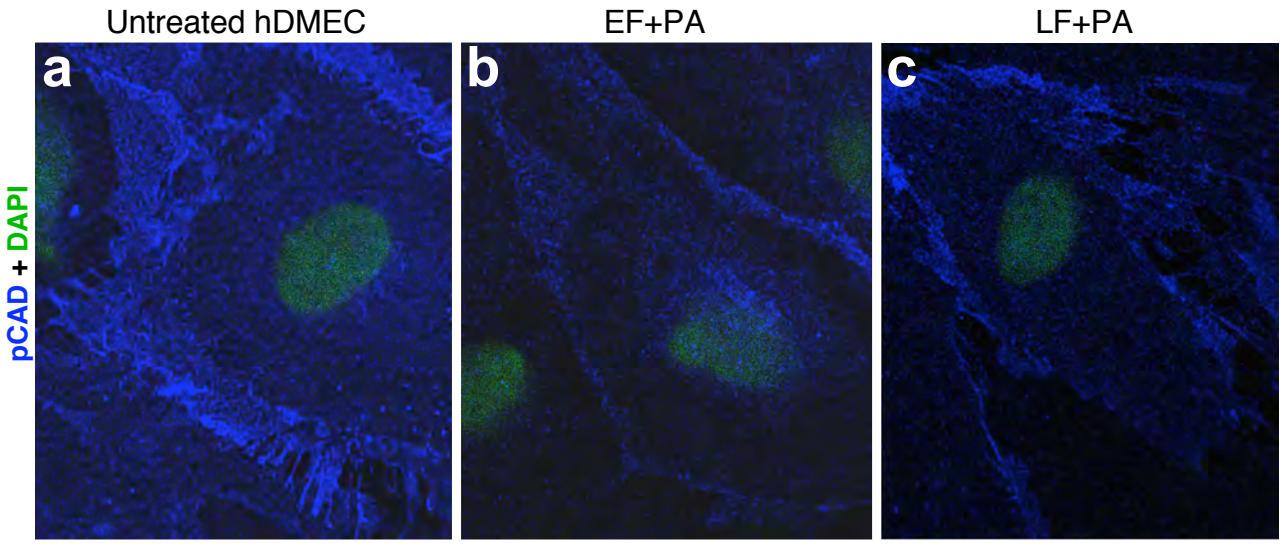

S10: Comparison of the effects of EF and LF on pCad staining in primary human dermal microvascular cells (hDMEC)

Untreated (**a**), EF toxin treated (**b**), and LF toxin treated (**c**) primary human dermal microvascular endothelial cells (hDMEC) were stained for pCad expression. EF toxin (1μg EF+PA) nearly eliminated pCad staining while, as in flies, LF toxin (3 μg LF+PA) treatment resulted in a moderate reduction. Similar modest effects of LF toxin on cadherin levels have been reported in other cells[1].

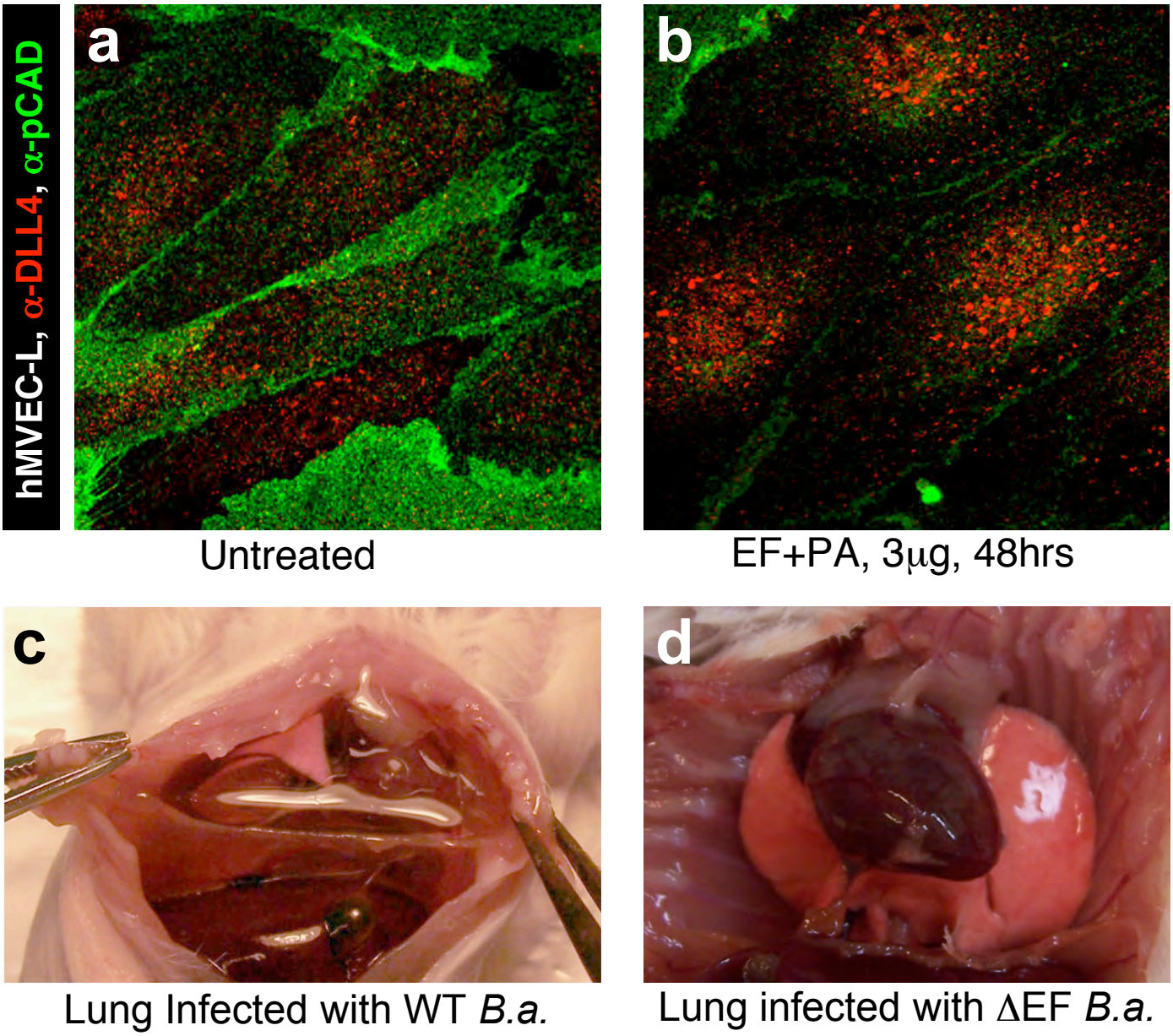

S11: EF blocks recycling of cadherins and Dll4 in primary lung cells and induces vascular effusion in the lung

a) Untreated primary human lung microvascular endothelial cells (hMVEC-L) express pCAD (green) at points of cell-cell contact and contain small regular shaped Dll4 staining vesicles (red). **b)** Treatment of hMVEC-L with EF toxin (3 μg EF+PA) for 48 hours resulted in a reduction of pCAD expression and enlarged Dll4 vesicles (i.e., the average Dll4 particle size increased 65% upon EF treatment, $p<0.001$). **c,d**) Pleural effusion is observed in the lungs of CD-1 mice infected with (**c**) the Sterne strain of *B. anthracis* (WT *B.a.*), but not in those infected with the (**d**) ΔEF mutant strain, despite these animals having similar titers of bacteria in the kidney (data not shown).

a qPCR quantitation of *Hes1* levels in Fig. 3n

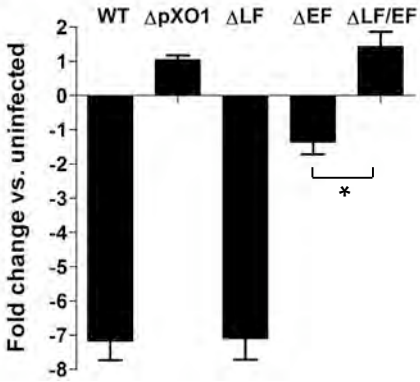

b qPCR quantitation of *RBPJ* levels

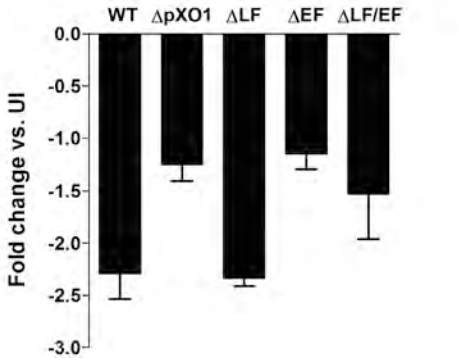

c Transwell assay for ET-induced leakage

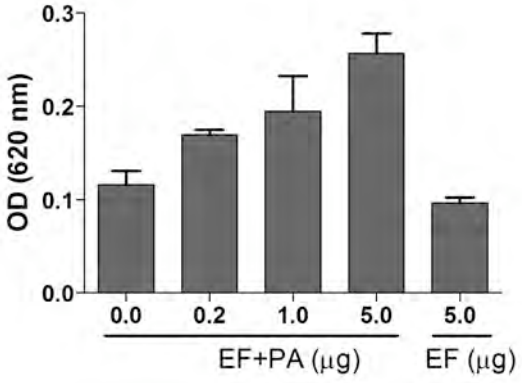

S12: Quantification of anthrax toxin effects

a) Quantitation of *Hes1* transcript levels in hBMEC infected with *B. anthracis* (WT) or isogenic toxin mutants measured by qPCR. *B. anthracis* genotypes are as described in **Fig. 4n**. Expression is normalized to GapDH and *Hes1* expression levels in uninfected hBMEC. Bars represent mean and Standard Deviatation (denoted by error bars) of three independent experiments.

b) Expression of a second known Notch target gene, RBJP, quantitated by qPCR. Bars represent mean and Standard Deviatation (denoted by error bars) of three independent experiments.

c) Dose-dependent effect of EF toxin on hBMEC permeability in a transwell assay. EF alone at the highest dose was used as a control. Results represent mean and Standard Deviatation (denoted by error bars) from a representative experiment.

Rab protein	BL# for RabDN	Wing phenotype in stgG4>RabDN	BL# for Rabwt	Wing phenotype in stgG4>Rabwt	Wing phenotype in stgG4>EF+Rabwt
Rab1	9757	100% lethal	24104	No phenotype	Semi lethal
Rab2	9759	No phenotype	23246	No phenotype	No effect on EF
Rab3	9766	No phenotype	9762	No phenotype	No effect on EF
Rab4	9768, 9769	No phenotype	23269 9767	No phenotype	No effect on EF
Rab5	9771, 9772	100% lethal	9775 24616	No phenotype	No effect on EF
Rab6	23249	No phenotype	23251	No phenotype	No effect on EF
Rab7	9778	No phenotype	23641	No phenotype	Mild enhancement
Rab8	23271	No phenotype	23272	No phenotype	No effect on EF
Rab9	23642	No phenotype	9783	No phenotype	No effect on EF
Rab10	9788	No phenotype	9789	Weak curvature	Mild enhancement
Rab11	**9792**	**EF-like phenotype**	**9790**	**No phenotype**	**Suppression of EF phenotype**
Rab14	23263	L2 and L3 thicker and closer	9793 9794	No phenotype	No effect on EF
Rab18	23237	No phenotype	9796	No phenotype	Weak suppression
Rab19	9799	No phenotype	24150	No phenotype	Enhancement
Rab21	23240	No phenotype	23242	Weak EF-like phenotype	Enhancement
Rab23	9804	No phenotype	9802	No phenotype	No effect on EF
Rab26	9807	No phenotype	23244	No phenotype	No effect on EF
Rab27	23267	No phenotype	9810	No phenotype	No effect on EF
Rab30	9813	No phenotype	9812	No phenotype	No effect on EF
Rab32	23281	No phenotype	23282	No phenotype	No effect on EF
Rab35	9819	Curved wings	9821	No phenotype	No effect on EF
Rab39	23247	No phenotype	9825	Lethal in males, Weak curvature	Weak enhancement
Rab40	9828	Curved wings	9830	No phenotype	No effect on EF
RabX1	9838	No phenotype	23274	No phenotype	No effect on EF
RabX2	9843	No phenotype	23275	No phenotype	Enhancement
RabX3	9845	No phenotype	23276	No phenotype	No effect on EF
RabX4	9849	No phenotype	9851	No phenotype	No effect on EF
RabX5	9853	No phenotype	9854	No phenotype	No effect on EF
RabX6	23253	No phenotype	23278	No phenotype	No effect on EF

Supplementary Table 1: Effects of expressing DN-Rabs in the *Drosophila* wing and the ability of wild-type Rabs to rescue the effects EF

Dominant negative (DN) forms of each *Drosophila* Rab protein were expressed in the wing using the MS1096 GAL4 driver (StgG4). Adult wing phenotypes were scored unless lethal. Only one, (Rab11DN), produced a Notch-like phenotype (**Fig. 2l**) resembling that caused by EF expression (**Fig. 2j**). In addition, wild-type (WT) forms of each Rab were expressed alone or co-expressed with EF with the same GAL4 driver. None of the WT Rabs caused any pronounced phenotype when expressed on their own and only one, WT Rab11, provided significant rescue of the EF phenotype (**Fig. 2p**).

Genotype/Antigen	Delta ratios	Rab11 ratios	Sec15 (particle ratios)
wt wing discs	$\overline{D/V}$ = 0.95±0.11 (N=8)	$\overline{D/V}$ = 0.97±0.08 (N=5) $\overline{A/B}$ = 3.5±0.96 (N=10)	N.A. (N=6)
StgG4>EF discs	$\overline{D/V}$ = 0.11±0.11**** (N=7) $\bar{D}$(EF)/$\bar{D}$(wt) = 0.18**** (N=7) $\bar{D}_t$(EF)/$\bar{D}_t$(wt) = 0.45** (N=7) $\bar{D}_a$(EF)/$\bar{D}_a$(wt) = 0.34* (N=7)	$\overline{D/V}$ = 0.43±0.09**** (N=4) $\overline{A/B}$ = 1.5±1.25** (N=10) $\bar{A}_t$(EF)/$\bar{A}_t$(wt) = 0.51*** (N=10) $\bar{B}_t$(EF)/$\bar{B}_t$(wt) = 1.24** (N=10)	$\bar{\#}$(EF)/$\bar{\#}$(wt) = 0.15**** (N=4) $\overline{size}$(EF)/$\overline{size}$(wt) = 0.55*** (N=4)
StgG4>LF discs	$\overline{D/V}$ = 0.32±0.11**** (N=8) $\bar{D}$(LF)/$\bar{D}$(wt) = 0.25** (N=8) $\bar{D}_t$(LF)/$\bar{D}_t$(wt) = 0.56* (N=8)	Not statisically different from wt	$\bar{\#}$(LF)/$\bar{\#}$(wt) = 0.28**** (N=5) $\overline{size}$(LF)/$\overline{size}$(wt) = 0.48**** (N=5)

Supplementary Table 2: Quantitation of staining ratios

Data presented in Figures 2 and 3 showing changes in expression of Dl, DE-Cad or pCAD, Rab11, Sec15-GFP in response to expression of EF or LF were quantitated using image J software to measure differences in levels of fluorescence intensity in wild-type/untreated cells versus cells expressing or exposed to toxins. We quantified these results in several ways. Gene expression levels in *Drosophila* wing discs presented in Figure 2 were obtained using the MS1096-GAL4 line, which drives expression of UAS-transgenes at much higher levels in cells on the dorsal surface than on the ventral surface. For these data, we measured the relative fluorescence on the dorsal versus ventral surfaces within individual wing discs and averaged these values across several wing discs. In wild-type discs, these values are close to one and were typically less than one in discs expressing either EF or LF. We also normalized these data with reference to tubulin or actin (phalloidin) staining within the same discs (e.g., LF and EF Dl stains). In addition, in some cases, we compared the total average fluorescence signals on the dorsal surfaces between wild-type and toxin expressing discs. We also determined the average size and number of vesicles/particles in several instances (e.g., Rab11 and Sec15-GFP). Similar quantitation of protein levels was performed for the expression data in human cells presented in Figure 3. Symbols in the table denote the following:

$\overline{D/V}$ = average ratio of staining in regions of fixed size on the dorsal versus ventral surface of the wing disc.

$\overline{D}$ = average staining in a region of fixed size on the dorsal surface of the wing disc.

$\overline{V}$ = average staining in a region of fixed size on the ventral surface of the wing disc.

$\overline{A/B}$ = average ratio of particle number in regions of fixed size in apical versus baso-lateral regions of Z-sections of the wing disc.

$\overline{A_t}$ = average staining relative to tubulin in an apical region of fixed size.

$\overline{B_t}$ = average staining relative to tubulin in a baso-lateral region of fixed size.

$\overline{\#}$ = average number of particles

$\overline{size}$ = average size of particles

± = Standard Deviation; N = number of discs; N.A. = not applicable; subscript t = normalized to tubulin; subscript a = normalized to actin (phalloidin); statistical significance in indicated by:
* $p<0.05$; ** $p<0.01$; *** $p<0.001$; **** $p<0.00001$.

With regard to human cells, we quantitated the number and size of Sec15-GFP particles as well as overall average signal intensity. There were an average of 86 particles per untreated cell (±44, N=6), 12 particles/EF toxin treated cell (±17, N=5), 8 particles/LF toxin treated cell (±7.8, N=6). The p-values for particle number were: EF/untreated, $p = 0.0064$, and for LF/untreated $p = 0.0016$. The average particle size in untreated cells was 62 pixels (±38, N=6), for EF toxin treated cells 9.4 pixels (±14.5, N=5), and for LF toxin treated cell 9.3 pixels (±9.4, N=6). The p-values for particle size were: EF/untreated, $p = 0.0081$; and LF/untreated $p = 0.016$. We also determined the ratio for overall average pixel intensity in a region of fixed size covering the cell for EF toxin treated/untreated cells = 0.46 ($p=0.0036$), and the same comparison normalized to tubulin = 0.45 ($p=0.005$); and for LF toxin treated/untreated cells = 0.37 ($p=0.0004$): N=11, untreated cells, N =10, EF toxin treated cells; N= 8, LF toxin treated cells.

Supplementary Results: LF and EF inhibit Notch signaling in *Drosophila*

Expression of LF along the wing margin causes notching (Supplementary Fig. 1b). Ubiquitous expression of LF also produced wing notching (data not shown) and other characteristic Notch phenotypes such as thickened veins (Supplementary Fig. 2a). These Notch-related phenotypes were superimposed upon an overall reduction in wing size resulting from inhibition of the MAPKK Dsor1[1] (Fig. 1l), and were the only non MAPKK-related phenotypes we observed upon expressing LF with a variety of other GAL4 drivers. Lower level expression of LF along the margin (in females) resulted in only occasional small notches (Supplementary Fig. 2d). However, consistent with LF acting on the Notch pathway, this modest effect of LF was greatly enhanced by a 50% reduction in *Notch* gene dosage (Supplementary Fig. 2e), which on its own also has only a mild phenotype (Supplementary Fig. 2b). Similarly, reducing the gene dose of the Notch ligand Delta (Dl), which alone has no effect on the margin (Supplementary Fig. 2c), increased the severity and frequency of LF-induced notching (Supplementary Fig. 2f, compare with Supplementary Fig. 1b). Consistent with its adult effects, LF reduced expression of Notch target genes such as *wingless* (*wg*) (Supplementary Fig. 1e), Cut (Supplementary Fig. 1h), and a synthetic Notch-reporter construct (data not shown) along the future wing margin in developing larval wing imaginal discs.

Expression of EF also resulted in Notch-like phenotypes consisting of a notched wing margin (Supplementary Fig. 1c), thickened veins (Fig. 1m; arrowhead), and missing thoracic bristles (Supplementary Fig. 4a,b). These EF phenotypes were stronger than those caused by LF driven by the same GAL4 drivers (e.g., Fig. 1e vs. 1f and Fig. 1l vs.

1m). As in the case of LF, Notch-like phenotypes caused by EF were strongly enhanced by reducing the levels of Notch pathway components such as in heterozygotes for *Notch* (Supplementary Fig. 2g,h) or *Delta* (*Dl*) (Supplementary Fig. 2g,i) loss-of-function alleles; conversely, EF induction of wing notching was suppressed by a constitutively active *Notch* allele (*N*[*Ab*], Supplementary Fig. 2j-l). In addition, a vein-loss phenotype caused by mis-expression of the Dl ligand in the second longitudinal vein primordium (Supplementary Fig 2m, arrowhead) was suppressed by co-expression with EF (Supplementary Fig. 2n, arrowhead). Also paralleling findings with LF, these EF-dependent adult phenotypes were presaged by defects in Notch signaling during larval development. For example, expression of EF in extreme anterior and posterior regions of the larval wing primordium (using the *brk*GAL4 driver) reduced expression of the Notch target genes *wg* (Supplementary Fig. 1d,f - bars) and Cut (Supplementary Fig. 1g,i - bars), as well as a *Notch* reporter construct (not shown). These peripheral regions of the developing wing margin ultimately give rise to areas of the adult wing exhibiting notches (Supplementary Fig. 1c - bars).

References:

1. Guichard, A., Park, J. M., Cruz-Moreno, B., Karin, M. & Bier, E. Anthrax Lethal Factor and Edema Factor act on conserved targets in *Drosophila*. Proc Natl Acad Sci U S A 103, 3244-9 (2006).

Microscopy Settings:
All confocal images were collected from a Leica SP2 microscope and were obtained using the same basic microscope settings, a specific example of which is provided below. The exact range of frequencies gated varied depending on the combination of fluorophores used in each experiments so as to exclude cross-contamination of signals from adjacent channels. These fluors included: Alexa 646, Alexa 555, Alexa 488, GFP, and DAPI. For some figure panels, the intensity, contrast, or brightness were altered to optimize the images, but in such cases, the alterations were performed over the entire image and the same adjustments were applied to all panels from the same experiment.

Leica Microsystems Heidelberg GmbH
Date: Monday, July 12, 2010
Time: 14:37

File Version: 26000000

EXPERIMENT INFORMATION
Type: Series with 'tif'-files

DIMENSION DESCRIPTION #0
Pixel Size in Byte: 1
Resolution in Bit: 8
Max Value: 255.0000000000
Min Value: 0.000000e+000
Label: I
Number of Dimensions: 3
Dimension_0: 120
Logical Size: 1024
Physical Length: 3.750000e-004 m
Physical Origin: 0.000000e+000 m
Dimension_1: 121
Logical Size: 1024
Physical Length: 3.750000e-004 m
Physical Origin: 0.000000e+000 m
Dimension_2: 6815843
Logical Size: 1
Physical Length: 0.000000e+000
Physical Origin: 0.000000e+000
Series Name: Image009
Description:

HARDWARE PARAMETER #0
AOBS (0) 100.000000
AOBS (1) 100.000000
AOBS (2) 0.000000

AOBS (3)	0.000000	
AOBS (4)	0.000000	
AOBS (5)	0.000000	
AOBS (6)	0.000000	
AOBS (7)	0.000000	
AOBS (0)	0.000000	
AOBS (1)	0.000000	
AOBS (2)	0.000000	
AOBS (3)	0.000000	
AOBS (4)	0.000000	
AOBS (5)	0.000000	
AOBS (6)	0.000000	
AOBS (7)	0.000000	
AOTF (458)	0.000000	
AOTF (476)	0.000000	
AOTF (488)	0.000000	
AOTF (514)	0.000000	
AOTF (543)	100.000000	
AOTF (633)	0.000000	
AOTF (458)	0.000000	
AOTF (476)	0.000000	
AOTF (488)	0.000000	
AOTF (514)	0.000000	
AOTF (543)	0.000000	
AOTF (633)	0.000000	
PMT 1	Inactive	Inactive
PMT 2	Active	Active
PMT 2 (Offs.)	-6.100000	
PMT 2 (HV)	548.651817	
PMT 3	Inactive	Inactive
PMT Trans	Inactive	Inactive
Beam Expander	Beam Exp 6	Beam Exp 6
Excitation FW UV	---	---
UV Lens FW	Lens 40x/1.25 Oil	Lens 40x/1.25 Oil
Hardware Type No.	2.000000	
Scan Field Rotation	-0.038943	
Rotation Direction	1	
X Scan Actuator	Active	Active
X Scan Actuator (Gain)	1.000000	
X Scan Actuator (Offs.)	0.000000	
Y Scan Actuator	Active	Active
Y Scan Actuator (Gain)	1.000000	
Y Scan Actuator (Offs.)	0.000000	
Z Scan Actuator	Inactive	Inactive
Z Scan Actuator (POS)	-0.000001	
Scan Speed	400.000000	

Phase 22.070313
Y-Phase 0.122100
SP Mirror 1 (left) 500.000000
SP Mirror 1 (right) 536.000000
SP Mirror 1 (stain) ALEXA 488 ALEXA 488
SP Mirror 2 (left) 550.000000
SP Mirror 2 (right) 625.000000
SP Mirror 2 (stain) ALEXA 555 ALEXA 555
SP Mirror 3 (left) 641.000000
SP Mirror 3 (right) 719.000000
SP Mirror 3 (stain) ALEXA 647 ALEXA 647
Objective HCX PL APO CS 40.0x1.25 OIL UV HCX PL APO CS 40.0x1.25 OIL UV
Order number (Obj.) 506179
Numerical aperture (Obj.) 1.250000

SCANNER INFORMATION #0
RoiScan 0
IsSequential 0
ChaserUVShutter 0
ChaserVisibleShutter 0
MPShutter 0
UVShutter 0
VisibleShutter 1
ScanMode xyz Inactive
Pinhole [m] 0.000081
Pinhole [airy] 0.998607
Size-Width [µm] 375.000000
Size-Height [µm] 375.000000
Size-Depth 0.000000
StepSize [µm] 0.040703
Voxel-Width [µm] 0.366211
Voxel-Height [µm] 0.366211
Voxel-Depth 0.000000
Zoom 1.000000
Scan-Direction 1
Y-Scan-Direction 1
SequentialMode 0
Frame-Accumulation 1
Frame-Average 1
Line-Average 4
Resolution 8
Channels 1
Format-Width 1024
Format-Height 1024
Sections 1

TIME INFORMATION #0
Stamped Dimension: 2
Stamp_0: 2010:07:12,13:39:25:109

LUT DESCRIPTION #0
LUT_0
Name: Red
Inverted (1=yes / 0=no): 0

SEQUENTIAL INFORMATION #0
Sequence Count: 0

SERIES INFORMATION #0
Number of Series: 51

IMAGES INFORMATION #0
Number of Images: 1
Image Width: 1024
Iamge Length: 1024
Bits per Sample: 8
Samples per Pixel: 1